SPANDIDOS PUBLICATIONS

BIOMEDICAL REPORTS 9: 175-180, 2018

Anti-proliferative effect of ridaifen-B on hepatoma cells

GO HASEGAWA[1], KOTOMI AKATSUKA[2], KEITA HIRUMA[3], KAYAKO SUDA[1], YUMIKO YOKOE[3], AKIHITO MIZUSAWA[3], NOZOMI OTA[3], NATSUMI SHIBATA[3], KAHO TSUCHIYA[2], MOYURU HAYASHI[1], ISAMU SHIINA[4] and MOTOYUKI SHIMONAKA[1]

[1]Department of Chemistry, Faculty of Science, Tokyo University of Science, Tokyo 162-8601; [2]Department of Chemistry, Graduate School of Science, Tokyo University of Science, Tokyo 162-8601; [3]Department of Chemical Sciences and Technology, Graduate School of Chemical Sciences and Technology, Tokyo University of Science, Tokyo 162-8601; [4]Department of Applied Chemistry, Faculty of Science, Tokyo University of Science, Tokyo 162-8601, Japan

Received April 11, 2018; Accepted June 12, 2018

DOI: 10.3892/br.2018.1112

Abstract. Ridaifens (RIDs), a novel series of tamoxifen derivatives, exhibit a potent growth-inhibitory effect against numerous tumor cells regardless of the expression of estrogen receptors, and are thus promising candidates as novel anti-tumor drugs. RID-B is a first generation RIDs, and inhibits the proliferation of several tumor cell lines. However, the potentially growth inhibitory effect of RID-B against hepatoma cells, and the detailed mechanism underlying RID-B-mediated tumor cell death remain to be elucidated. The purpose of the current study was to evaluate the anti-proliferative effect of RID-B against hepatoma cells. The anti-proliferative effect of RID-B against human hepatoma Huh-7 cells was investigated by cell proliferation assay using WST-1 reagent, and caspase-3 activity was evaluated by using specific fluorescent substrate. In addition, DNA fragmentation in Huh-7 cells induced by RID-B was estimated by terminal deoxynucleotidyl transferase dUTP nick-end labelling assay, and binding of RID-B to double-stranded DNA was confirmed by mass spectrometry. RID-B (0.5, 1 and 2 μM) inhibited the growth of Huh-7 cells, seemingly dose-dependently, but did not inhibit the growth of normal primary rat hepatocytes in the same concentration range. Furthermore, the caspase-3 activity of Huh-7 cells was increased by RID-B (0.5 and 5 μM), and the anti-proliferative effect of RID-B (1 μM) on Huh-7 cells was partially suppressed by the addition of the caspase inhibitor, Z-VAD-FMK. Additionally, RID-B (10 μM) directly bound to double-stranded DNA, and the addition of DNA suppressed RID-B-mediated cell growth inhibition and DNA fragmentation in Huh-7 cells. From these data, it may be concluded that RID-B inhibited cell growth and induced apoptosis via activating caspase-3 and binding to DNA directly, leading to DNA fragmentation in hepatoma cells.

Correspondence to: Dr Motoyuki Shimonaka, Department of Chemistry, Faculty of Science, Tokyo University of Science, 1-3 Kagurazaka, Shinjuku-ku, Tokyo 162-8601, Japan
E-mail: simonaka@rs.kagu.tus.ac.jp

Key words: ridaifen, tamoxifen derivative, hepatoma, growth inhibition, apoptosis, caspase, DNA binding

Introduction

Ridaifens (RIDs) are novel tamoxifen derivatives (1,2). First generation RIDs possess common triphenylethylene structure, which is similar to tamoxifen, and various amine side chains connected to para-positions of the aromatic rings. Although tamoxifen reportedly induces anti-tumor effects by competitive inhibition of estrogen receptors (ERs) expressed in tumor cells, RIDs exhibit a growth-inhibitory effect on numerous tumor cell types regardless of the expression of ERs, suggesting that the mechanism underlying the anti-tumor effect of RIDs differs from that of tamoxifen (3). In previous study, among 48 RIDs, 40 exhibited greater growth inhibitory effect than tamoxifen, which was evaluated by a JFCR39 panel assay of 39 tumor cell lines, including breast cancer, glioma, colorectal cancer, lung cancer, melanoma, ovarian cancer, renal cancer, gastric cancer and prostate cancer (4). Furthermore, the mechanism of RID-mediated cancer cell growth inhibition may differ from that of currently used anti-cancer drugs, indicated by COMPARE analysis (4). One of the RIDs, RID-G, could induce caspase-independent atypical cell death involving mitochondrial dysfunction in human neoplastic hematopoietic cell lines (5), and has been indicated to interact with calmodulin, heterogeneous nuclear ribonucleoproteins A2/B1 and zinc finger protein 638 during its cancer cell growth inhibition (6). RID-F may serve as a proteasome inhibitor, and inhibit chymotrypsin-like, trypsin-like and peptidylglutamyl peptide hydrolase activities (7,8). These findings suggest that the various mechanisms of RID-mediated cancer cell growth inhibition should be considered in future study.

Anti-cancer drugs and their metabolites work through various mechanisms to induce damage to cancer cells. Certain metabolites of 5-fluorouracil disrupt RNA function by misincorporation into RNA and/or cause DNA damage by binding thymidylate synthase (9), while cisplatin crosslinks DNA by binding to guanines bases (10). These findings suggest the

possibility of binding of RID-B and double-stranded DNA in cancer cells.

RID-B (1,1-bis[4-[2-(pyrrolidin-1-yl)ethoxy] phenyl]-2-phenyl-1-butene), one of the first generation RIDs, contains pyrrolidine rings at the end of its alkyl side chains (Fig. 1), and has been observed to elicit marked cellular damage against both ER-positive and -negative tumor cells (11). It has also been reported that RID-B induces autophagy in the ER-negative human leukemia Jurkat cell line (12). RID-B may bind to Grb10 interacting GYF protein 2 (GIGYF2) and inhibits GIGYF2-mediated Akt phosphorylation (13). By previous JFCR39 panel assay, it was determined that the mean value of the concentration at which cell growth was inhibited by 50% (GI_{50}; designated as MG-MID) of RID-B was 1.17 μM, which was 6.3 times lower than the MG-MID of tamoxifen (4). However, to the best of our knowledge, the anti-proliferative effect of RID-B on hepatoma cells has not yet been investigated. Therefore, the aim of the current study was to evaluate the anti-proliferative effect of RID-B on hepatoma cells. The mechanism underlying the anti-proliferative effect of RID-B was also examined.

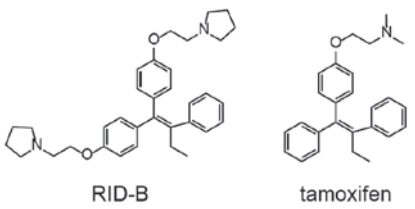

Figure 1. Chemical structures of RID-B and tamoxifen. RID-B, ridaifen-B.

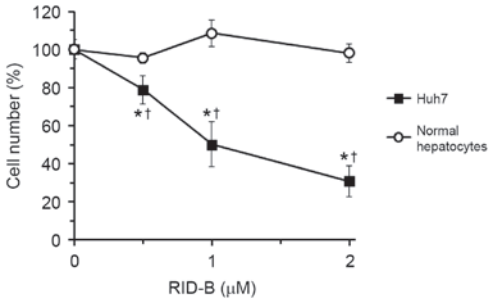

Figure 2. Anti-proliferative effect of RID-B on Huh-7 cells. Huh-7 cells and normal primary rat hepatocytes were incubated with RID-B for 48 h, and cell number was estimated by WST-1 assay. The number of cell at the control condition (RID-B, 0 μM) for each group was set as 100%, and the cell counts for all treatment groups were expressed as a percentage against the control. Values are presented as the mean ± standard deviation from four independent experiments performed in triplicate. Two-way analysis of variance followed by Tukey's post-hoc testing was used for comparison among groups. *P<0.05 vs. 0 μM RID-B; †P<0.05 vs. normal hepatocytes at the same concentration. RID-B, ridaifen-B.

Materials and methods

Materials. RID-B was synthesized as described previously (1,2). Z-VAD-FMK, the caspase-1 and -3 inhibitor, was purchased from Promega Corporation (Madison, WI, USA), and all other general reagents not specified in the following text were purchased from Sigma-Aldrich (Merck KGaA, Darmstadt, Germany), Kanto Chemical Co., Inc. (Tokyo, Japan), Nacalai Tesque, Inc. (Kyoto, Japan) and Wako Pure Chemical Industries, Ltd. (Osaka, Japan).

Preparation of normal primary rat hepatocytes. Female Sprague-Dawley rats aged 8 weeks (n=3; weight range, 150-190 g) were obtained from Sankyo Labo Service Corporation, Inc. (Tokyo, Japan). The animals were housed in individual cages supplied with HEPA-filtered air. The ambient temperature in the animal room was maintained at 23±1˚C, and the relative humidity at 50-60%. A 12-h light/dark cycle was maintained in the animal room, and food and water were provided *ad libitum*.

Rat hepatocytes were isolated as described previously (14-16) with some modifications. The liver of the anesthetized rats was perfused in situ via a cannulation of the portal vein. The liver was perfused for calcium removal with 50 ml of 10 mM 4-(2-hydroxyethyl)-1-piperazineethanesulfonic acid buffer containing 3.6 mM $NaHCO_3$, 5.6 mM glucose and 6.0 mM EGTA, following collagenase perfusion with 50 ml phosphate-buffered saline (PBS) containing 0.5 mg/ml collagenase, 4 mM $NaHCO_3$, 0.9 mM $MgSO_4$ and 4.5 mM $CaCl_2$. The hepatocytes were dispersed and washed three times with Dulbecco's modified Eagle's medium (DMEM) supplemented with antibiotic-antimycotic (100 U/ml penicillin, 100 μg/ml streptomycin, 0.25 μg/ml amphotericin B; Thermo Fisher Scientific, Inc., Waltham, MA, USA) and gentamicin (10 μg/ml, Thermo Fisher Scientific, Inc.). Cells were then resuspended with DMEM supplemented with antibiotic-antimycotic (100 U/ml penicillin, 100 μg/ml streptomycin, 0.25 μg/ml amphotericin B), gentamicin (10 μg/ml) and 10% heat-inactivated fetal bovine serum (FBS), and seeded into 96-well plates (1,000 cells/well). After 24 h of incubation at 37˚C with 5% CO_2, the culture medium was replenished, and cells were used for a proliferation assay. All animal procedures were conducted according to a protocol approved by the Tokyo University of Science Institutional Animal Care and Use Committee (Tokyo, Japan).

Cell proliferation assay. Human hepatoma Huh-7 cells (Japanese Collection of Research Bioresources Cell Bank, Osaka, Japan) were maintained at 37˚C with 5% CO_2 in DMEM supplemented with antibiotic-antimycotic (100 U/ml penicillin, 100 μg/ml streptomycin, 0.25 μg/ml amphotericin B), gentamicin (10 μg/ml) and 10% heat-inactivated FBS. Cells of passage number 70-80 were used throughout the study. Cells were grew to confluence for 2 days following passage.

The Huh-7 cells and normal primary rat hepatocytes were seeded in 96-well plates (1,000 cells/well) and incubated for 24 h at 37˚C. Cells were then incubated with RID-B (0.5, 1 and 2 μM) for 48 h, and cell number was estimated by using WST-1 cell proliferation reagent (Cell Counting Kit; Dojindo Molecular Technologies, Inc., Kumamoto, Japan) according to the manufacturer's protocol. The GI_{50} value of RID-B was calculated using JMP 9 software (SAS Institute, Inc., Cary, NC, USA) using the 4-parameter logistic model (17).

Plasmid DNA and salmon sperm DNA were used subsequently to competitively inhibit the effect of RID-B on Huh-7 cells. Huh-7 cells were seeded in 24-well plates ($4x10^4$ cells/well) and incubated for 24 h. Cells were then incubated

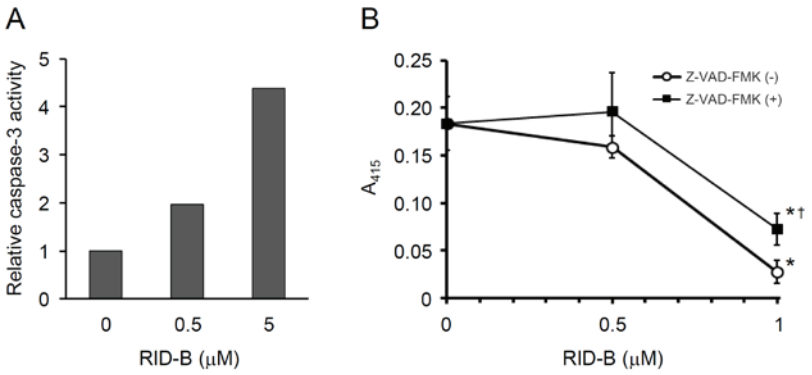

Figure 3. RID-B induces apoptosis in Huh-7 cells. (A) Huh-7 cells were incubated with RID-B for 24 h, and caspase-3 activity in RID-B-treated Huh-7 cell lysate was measured with fluorescent caspase-3 substrate (0.1 mM). Relative activity given as fold-change against the control (0 μM) is shown. The data shown are from one experiment representative of at least three separate experiments. (B) Huh-7 cells were pre-incubated with or without 10 μM caspase inhibitor, Z-VAD-FMK, for 2 h and cells were then incubated with RID-B for 48 h. Cell number was estimated by WST-1 assay. Values are the mean ± standard deviation from four independent experiments performed in triplicate. Two-way analysis of variance followed by Tukey's post-hoc test was used for comparison among groups. *P<0.05 vs. 0 μM RID-B; †P<0.05 vs. Z-VAD-FMK (-) at the same concentration. RID-B, ridaifen-B.

with RID-B (1 μM) in the presence of pSecTag2B plasmid DNA (0.125, 0.25 and 0.5 mg/ml, respectively; Thermo Fisher Scientific, Inc.) or salmon sperm DNA (0.125, 0.25 and 0.5 mg/ml, respectively; Wako Pure Chemical Industries, Ltd.) overnight at 37˚C. Following incubation, cells were stained with trypan blue and live cells were counted immediately under a Nikon TMS Inverted Microscope (Nikon Corporation, Tokyo, Japan) using a Neubauer hemocytometer. The number of cells was determined as the mean of all live cells counted in eight fields (0.1 mm^3/field) of view.

Determination of caspase-3 activity. Huh-7 cells were seeded in 24-well plates ($8x10^4$ cells/well) and incubated for 24 h at 37˚C. Cells were then incubated with RID-B (0.5 and 5 μM) for 24 h at 37˚C. Following incubation, cells were washed with PBS and lysed with 10 mM phosphate containing 0.15 M NaCl, 5 mM EDTA, 0.1% Nonidet P-40, 0.1% SDS and 0.1% sodium deoxycholate. Cell lysate was incubated with 0.1 mM caspase-3 substrate (acetyl-Asp-Glu-Val-Asp-4-methyl-coum aryl-7-amide; Peptide Institute, Inc., Osaka, Japan) for 3 min at room temperature, and the increase of fluorescence intensity was monitored by using an FP-6200 spectrofluorometer ($\lambda_{excitation}$ =380 nm, $\lambda_{emission}$ =460 nm; JASCO Corporation, Tokyo, Japan).

Terminal deoxynucleotidyl transferase dUTP nick-end labelling (TUNEL) assay. Huh-7 cells were seeded on 8-well culture slides ($4x10^4$ cells/well, BD Biosciences, San Jose, CA, USA) and cultured for 24 h at 37˚C. Following cultivation, cells were pre-incubated with or without 40 μM Z-VAD-FMK for 2 h at 37˚C, and were then incubated with RID-B (1 μM) in the presence or absence of 0.5 mg/ml pSecTag2B for 24 h at 37˚C. Following a thorough wash with PBS, cells were fixed with 3.7% formaldehyde/PBS for 30 min at room temperature and permeabilized with 0.1% sodium citrate containing 0.1% Triton X-100 for 2 min on ice. Cells were stained using a MEBSTAIN Apoptosis TUNEL Kit Direct (Medical and Biological Laboratories Co., Ltd., Nagoya, Japan), and TUNEL-positive cells were visualized by confocal laser scanning microscopy (LSM710; Carl Zeiss AG, Oberkochen, Germany).

Detection of RID-B and double-stranded DNA binding. For the preparation of biotinylated double-stranded DNA, complementary oligonucleotides (biotin-TTTTTTATATAT and ATATATAAAAAA; 1 μg/ml each) in distilled water were annealed for 30 min at 25˚C. The double-stranded DNA was incubated with RID-B (10 μM) in distilled water for 1.5 h at room temperature, and the reaction product was then incubated with streptoavidin-conjugated magnetic beads (APRO Science, Tokushima, Japan) for 1 h at room temperature. Magnetic beads were washed three times with distilled water to remove RID-B unbound to DNA, and the beads were then boiled for 5 min to separate RID-B from DNA. The supernatant containing RID-B was collected in a 4-tube magnetic rack (Bio-Rad Laboratories, Inc., Hercules, CA, USA). Betaine (5 μg/ml) was added to the supernatant for internal standard, and RID-B, which had bound to DNA, was detected by electrospray ionization time-of-flight mass spectrometry (ESI-TOF-MS; micrOTOF-NR-focus; Bruker Daltonik GmbH, Bremen, Germany). The mass spectrometer settings were as follows: Ionization mode, positive; nitrogen gas temperature, 180˚C; nebulizer pressure, 5.8 psi; flow rate: 4.0 l/min. The calculated mass ($M+H^+$) for $C_{34}H_{43}N_2O_2$ (RID-B) is 511.3319; the mass for RID-B identified in the experiments was 511.3628 (positive control) and 511.3584 (DNA (+)), respectively. The calculated mass ($M+H^+$) for $C_5H_{11}NO_2$ (betaine) is 118.0868; the mass for betaine identified in the experiments was 118.0991 (positive control), 118.0988 (DNA (+)) and 118.0976 (DNA (-)), respectively.

Statistical analysis. Data are expressed as the mean ± standard deviation. All experiments were performed at least three times. Two-way analysis of variance with Fisher's protected least significant difference was employed to compare mean values between groups. P<0.05 was considered to indicate a statistically significant difference. Data analysis was performed using JMP 9 software.

Results

RID-B inhibits the growth of human hepatoma Huh-7 cells but not normal primary rat hepatocytes. To evaluate the

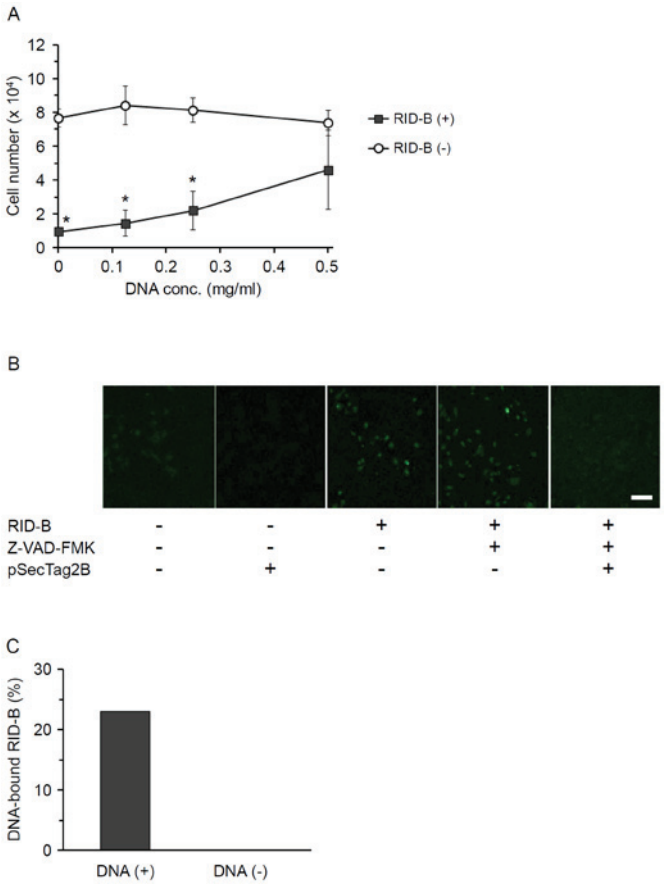

Figure 4. DNA inhibits the anti-proliferative effect of RID-B. (A) Huh-7 cells were incubated with or without 1 μM RID-B in the presence of plasmid DNA (pSecTag2B) overnight at 37˚C. Cells were then stained with trypan blue and live cells were counted. Values are the mean ± standard deviation from three independent experiments performed in triplicate. Two-way analysis of variance followed by Tukey's post-hoc test was used for comparison among groups. (B) Huh-7 cells were pre-incubated with or without 40 μM Z-VAD-FMK for 2 h and cells were then incubated with RID-B (1 μM) in the presence or absence of pSecTag2B for 24 h. Cells positive for terminal deoxynucleotidyl transferase dUTP nick-end labelling were visualized by confocal laser scanning microscopy (magnification, x100; scale bar, 100 μM). The data shown are from one experiment representative of at least three separate experiments. (C) RID-B (10 μM) was incubated with or without biotinylated double-stranded DNA for 1.5 h at room temperature. DNA-bound RID-B was then collected by streptoavidin-conjugated magnetic beads, and RID-B and DNA were separated by boiling. The ratio of DNA-bound RID-B was estimated by ESI-TOF-MS using betaine as the internal standard. The data shown are from one experiment representative of at least three separate experiments. *P<0.05 vs. RID-B (-). RID-B, ridaifen-B.

anti-proliferative effect of RID-B in hepatoma cells, human hepatoma Huh-7 cells and normal primary rat hepatocytes were incubated with RID-B, and cell numbers were estimated using WST-1 reagent (Fig. 2). Previous study indicated that the mean GI_{50}, for RID-B in 39 human cancer cell lines was 1.17 μM (4). Therefore, the RID-B concentration range of 0.5-2 μM was selected in the current study. RID-B inhibited the growth of Huh-7 cells between the concentrations of 0.5-2 μM (P<0.05 vs. 0 μM RID-B), in an apparent dose-dependent manner; however, RID-B did not inhibit the growth of normal hepatocytes within the same range. The GI_{50} of RID-B in Huh-7 cells was 1.00±0.16 μM. The GI_{50} of RID-B in rat hepatocytes could not be calculated as cell number did not fall below 90% (Fig. 2) and was therefore estimated as >2 μM. These results suggested that RID-B was more effective at inhibiting the growth of hepatoma cells than normal hepatocytes.

RID-B induces apoptosis in Huh-7 cells. To clarify the mechanism of cancer cell growth inhibition by RID-B, the effect of caspase inhibitor, Z-VAD-FMK, on RID-B-mediated cell growth inhibition was examined. As depicted in Fig. 3A, the caspase-3 activity of Huh-7 cells was apparently increased dose-dependently between the RID-B concentrations 0.5 and 5 μM. Furthermore, by the pretreatment with Z-VAD-FMK, RID-B-mediated Huh-7 cell growth was significantly attenuated at the RID-B concentration of 1 μM (P<0.05; Fig. 3B). It appears evident from these data that RID-B induced the apoptosis of Huh-7 cells via the activation of caspase-3.

Involvement of RID-B and DNA binding in Huh-7 cell apoptosis. To clarify the mechanism of RID-B-induced apoptosis in cancer cells, the effect of DNA on RID-B-mediated Huh-7 cell growth inhibition was examined. Huh-7 cells were incubated with RID-B in the presence of plasmid DNA (pSecTag2B), and live cells were then counted (Fig. 4A). The addition of plasmid DNA suppressed RID-B-mediated Huh-7 cell growth inhibition; notably, this competitive inhibition by plasmid DNA appeared dose-dependent, as no significant difference was identified between the number of Huh-7 cells incubated with and without RID-B at the DNA concentration of 0.5 mg/ml. Similar results were observed when using salmon sperm DNA instead of plasmid DNA in the same DNA concentration range (data not shown). From these data, it may be suggested that RID-B binds to DNA to induce cancer cell apoptosis.

As in Fig. 3, RID-B induced apoptosis in Huh-7 cells seemingly via the activation of caspase-3. To confirm whether DNA inhibited RID-B-induced apoptosis in cancer cells, Huh-7 cells were pre-incubated with Z-VAD-FMK, and the cells were then incubated with RID-B in the presence of plasmid DNA. By TUNEL assay, it was observed that RID-B caused DNA fragmentation of Huh-7 cells, suggesting that RID-B induced cancer cell apoptosis by causing DNA fragmentation. Z-VAD-FMK had no obvious effect on DNA fragmentation in RID-B-treated Huh-7 cells; whereas the addition of plasmid DNA appeared to completely suppress DNA fragmentation (Fig. 4B).

From the data in Fig. 4A and B, it was apparent that RID-B directly bound to DNA. To verify this hypothesis, RID-B was incubated with biotinylated double-stranded DNA, and DNA-bound RID-B was then collected by streptoavidin-conjugated magnetic beads. DNA-bound RID-B was detected by ESI-TOF-MS (Fig. 4C). The peak derived from RID-B was detected only from the sample incubated with double-stranded DNA, and not from that incubated without DNA, indicating that RID-B directly bound to double-stranded DNA. The ratio of RID-B bound to DNA was 23.0%.

Discussion

In the present study, the anti-proliferative effect of RID-B on human hepatoma Huh-7 cells was evaluated. Although RID-B did not inhibit the proliferation of rat primary normal hepatocytes, RID-B inhibited cell growth and induced apoptosis seemingly by activating caspase-3 and inducing DNA fragmentation in Huh-7 cells. The binding

of RID-B to double-stranded DNA indicated that RID-B may directly interact with genomic DNA. To the best of our knowledge, this is the first paper to report that RID-B could directly bind to DNA. Although the detailed mechanism for RID-B-mediated cancer cell growth inhibition and apoptosis is unknown, the following mechanism was indicated from the present findings: RID-B may activate caspase-3 to induce DNA fragmentation, and RID-B may directly bind to DNA to inhibit DNA synthesis. It has been reported that RID-B reduced mitochondrial membrane potential during the induction of apoptosis in the human lymphoid helper T-cell line Jurkat (11), and that RID-B induced microtubule-associated protein 1A/1B-light chain 3 and lysosome colocalization resulting in autophagy in Jurkat cells (12). Additionally, the current data revealed that caspase inhibitor, Z-VAD-FMK, partially suppressed RID-B-mediated growth inhibition and DNA fragmentation in Huh-7 cells. Taken together, the findings indicate the presence of diverse pathways involved in RID-B-mediated cancer cell growth inhibition and apoptosis. Since RID-B also influenced the proliferation of Huh-7 cells, our group is now investigating the effects of RID-B on the cell cycle.

Additionally, the results indicated that hepatoma cells were more sensitive to RID-B compared with normal rat hepatocytes. It has been reported that RID-SB8 preferentially induced cell death in human breast cancer cell lines, MCF-7 and MDA-MB-231, over normal human mammary epithelial cells (18). Although the detailed mechanism for the anti-proliferative effect of RID-B on cancer cells is as yet unclear, the efficacy of RID-B may be dependent on cell growth rate. Cancer cells generally grow more rapidly than normal cells, and the rate of DNA replication is particularly elevated in these cells (19). DNA is unstable in its replication process (20), and thus RID-B may more easily bind to DNA in cancer cells than in normal cells, causing cancer cell death. Taken together, it may be proposed that cancer cells are more sensitive to RIDs compared with normal cells.

The current study used primary rat hepatocytes as a normal counterpart for comparison of the anti-proliferative effect of RID-B on the human hepatoma Huh-7 line. Although human cell lines of normal hepatocytes, THLE-2 and THLE-3, express some phenotypic characteristics of normal adult liver epithelial cells, these cells were established as immortal lines by infection with simian virus 40 (SV40) large T antigen (21). SV40 large T antigen-transfected cell lines usually exhibit enhanced proliferative rate compared with primary normal cells (22,23), suggesting that the proliferative characteristics of SV40 large T antigen-transfected cells may differ markedly from that of primary normal cells. For these reasons, primary rat hepatocytes appeared more appropriate than immortalized human hepatocyte cell lines as a normal counterpart in the current study. The detailed mechanism of cancer cell death induced by RID-B will be investigated further in our upcoming studies.

In conclusion, the results of the current study indicate that RID-B may be useful as a liver cancer therapeutic, by inducing apoptosis via activation of caspase-3 and directly binding to DNA to lead to DNA fragmentation. The current data further suggest that RID-B affects hepatoma cells without or with little side-effect against normal cells. Further studies are required to validate its effectiveness and safety in prospective clinical application as a liver cancer therapy.

Acknowledgements

The authors thank Professor Yukitoshi Nagahara (Division of Life Science and Engineering, School of Science and Engineering, Tokyo Denki University, Tokyo, Japan) for their advice and sharing of materials throughout this study.

Funding

The current study was supported by a Health and Labour Sciences Research Grant from the Ministry of Health, Labour and Welfare, Japan (grant no. 11103425 to IS).

Availability of data and materials

The datasets used and/or analyzed during this study are available from the corresponding author on reasonable request.

Authors' contributions

GH and MS designed the study. AM, NO, NS, KT and IS synthesized RID-B. GH, KA, KH, KS, YY and MH performed the cell proliferation assay. KH measured caspase-3 activity. KS conducted the TUNEL assay. GH, KA, YY, AM, NO and IS performed the RID-B-DNA binding assay. GH analyzed the data. GH, IS and MS wrote the manuscript. All authors read and approved the final version of the manuscript.

Ethics approval and consent to participate

All animal procedures were conducted by a protocol approved by the Tokyo University of Science Institutional Animal Care and Use Committee (Tokyo, Japan).

Consent for publication

Not applicable.

Competing interests

The authors declare that they have no competing interests.

References

1. Shiina I, Sano Y, Nakata K, Kikuchi T, Sasaki A, Ikekita M and Hasome Y: Synthesis of the new pseudo-symmetrical tamoxifen derivatives and their anti-tumor activity. Bioorg Med Chem Lett 17: 2421-2424, 2007.
2. Shiina I, Sano Y, Nakata K, Kikuchi T, Sasaki A, Ikekita M, Nagahara Y, Hasome Y, Yamori T and Yamazaki K: Synthesis and pharmacological evaluation of the novel pseudo-symmetrical tamoxifen derivatives as anti-tumor agents. Biochem Pharmacol 75: 1014-1026, 2008.
3. Shagufta and Ahmad I: Tamoxifen a pioneering drug: An update on the therapeutic potential of tamoxifen derivatives. Eur J Med Chem 143: 515-531, 2018.
4. Guo WZ, Wang Y, Umeda E, Shiina I, Dan S and Yamori T: Search for novel anti-tumor agents from ridaifens using JFCR39, a panel of human cancer cell lines. Biol Pharm Bull 36: 1008-1016, 2013.
5. Anlifeire A, Hatori M, Morita A, Shiina I, Nakata K, Tosaki Y, Wang Y-W, Ikekita M and Li G: Ridaifen G induces caspase independent atypical cell death. Chin J Cell Biol 33: 635-644, 2011.

6. Ikeda K, Kamisuki S, Uetake S, Mizusawa A, Ota N, Sasaki T, Tsukuda S, Kusayanagi T, Takakusagi Y, Morohashi K, *et al*: Ridaifen G, tamoxifen analog, is a potent anticancer drug working through a combinatorial association with multiple cellular factors. Bioorg Med Chem 23: 6118-6124, 2015.
7. Hasegawa M, Yasuda Y, Tanaka M, Nakata K, Umeda E, Wang Y, Watanabe C, Uetake S, Kunoh T, Shionyu M, *et al*: A novel tamoxifen derivative, ridaifen-F, is a nonpeptidic small-molecule proteasome inhibitor. Eur J Med Chem 71: 290-305, 2014.
8. Tanaka M, Zhu Y, Shionyu M, Ota N, Shibata N, Watanabe C, Mizusawa A, Sasaki R, Mizukami T, Shiina I, *et al*: Ridaifen-F conjugated with cell-penetrating peptides inhibits intracellular proteasome activities and induces drug-resistant cell death. Eur J Med Chem 146: 636-650, 2018.
9. Longley DB, Harkin DP and Johnston PG: 5-fluorouracil: Mechanisms of action and clinical strategies. Nat Rev Cancer 3: 330-338, 2003.
10. Todd RC and Lippard SJ: Inhibition of transcription by platinum antitumor compounds. Metallomics 1: 280-291, 2009.
11. Nagahara Y, Shiina I, Nakata K, Sasaki A, Miyamoto T and Ikekita M: Induction of mitochondria-involved apoptosis in estrogen receptor-negative cells by a novel tamoxifen derivative, ridaifen-B. Cancer Sci 99: 608-614, 2008.
12. Nagahara Y, Takeyoshi M, Sakemoto S, Shiina I, Nakata K, Fujimori K, Wang Y, Umeda E, Watanabe C, Uetake S, *et al*: Novel tamoxifen derivative Ridaifen-B induces Bcl-2 independent autophagy without estrogen receptor involvement. Biochem Biophys Res Commun 435: 657-663, 2013.
13. Tsukuda S, Kusayanagi T, Umeda E, Watanabe C, Tosaki YT, Kamisuki S, Takeuchi T, Takakusagi Y, Shiina I and Sugawara F: Ridaifen B, a tamoxifen derivative, directly binds to Grb10 interacting GYF protein 2. Bioorg Med Chem 21: 311-320, 2013.
14. Seglen PO: Preparation of isolated rat liver cells. Methods Cell Biol 13: 29-83, 1976.
15. Quistorff B, Dich J and Grunnet N: Preparation of Isolated Rat Liver Hepatocytes. In: Animal Cell Culture. Walker JM and Pollard JW (eds). Humana Press, Totowa, NJ, pp151-160, 1990.
16. Francavilla A, Ove P, Polimeno L, Sciascia C, Coetzee ML and Starzl TE: Epidermal growth factor and proliferation in rat hepatocytes in primary culture isolated at different times after partial hepatectomy. Cancer Res 46: 1318-1323, 1986.
17. Sebaugh JL: Guidelines for accurate EC50/IC50 estimation. Pharm Stat 10: 128-134, 2011.
18. Guo WZ, Shiina I, Wang Y, Umeda E, Watanabe C, Uetake S, Ohashi Y, Yamori T and Dan S: Ridaifen-SB8, a novel tamoxifen derivative, induces apoptosis via reactive oxygen species-dependent signaling pathway. Biochem Pharmacol 86: 1272-1284, 2013.
19. Fadaka A, Ajiboye B, Ojo O, Adewale O, Olayide I and Emuowhochere R: Biology of glucose metabolization in cancer cells. J Oncol Sci 3: 45-51, 2017.
20. Jeggo PA, Pearl LH and Carr AM: DNA repair, genome stability and cancer: A historical perspective. Nat Rev Cancer 16: 35-42, 2016.
21. Pfeifer AM, Cole KE, Smoot DT, Weston A, Groopman JD, Shields PG, Vignaud JM, Juillerat M, Lipsky MM and Trump BF: Simian virus 40 large tumor antigen-immortalized normal human liver epithelial cells express hepatocyte characteristics and metabolize chemical carcinogens. Proc Natl Acad Sci USA 90: 5123-5127, 1993.
22. Reddel RR, De Silva R, Duncan EL, Rogan EM, Whitaker NJ, Zahra DG, Ke Y, McMenamin MG, Gerwin BI and Harris CC: SV40-induced immortalization and ras-transformation of human bronchial epithelial cells. Int J Cancer 61: 199-205, 1995.
23. Martin RG and Oppenheim A: Initiation points for DNA replication in nontransformed and simian virus 40-transformed Chinese hamster lung cells. Cell 11: 859-869, 1977.